Supporting Information

Structure modification and luminescence regulation in new violet light excitable $Sr_{(2-y)}Ba_yY_4La_4(SiO_4)_6O_2$:$x$$Eu^{2+}$ phosphors via cation substitution

Jie Zhang,[a] Langping Dong,[a *] Feng Wang[b] Jingshan Hou,[a *] and Yongzheng Fang[a *]

[a] *School of Materials Science and Engineering, Shanghai Institute of Technology, Shanghai, 201418, China.*

[b] *Department of Materials Science and Engineering, City University of Hong Kong, 83 Tat Chee Avenue, Hong Kong SAR, China*

*Corresponding author. *E-mail address:* lpdong@sit.edu.cn (L. P. D.); houjingshan@hotmail.com (J. S. H.); fyz1003@sina.com (Y. Z. F.).

Table S1. Crystallographic data and refined parameters for the $Sr_{(2-y)}Ba_yY_4La_4(SiO_4)_6O_2$:$Eu^{2+}$ ($0.5 \leq y \leq 2$) samples.

Sample	Sr_2	$Sr_{1.5}Ba_{0.5}$	SrBa	$Sr_{0.5}Ba_{1.5}$	Ba_2
Space group	*P6₃/m*	*P6₃/m*	*P6₃/m*	*P6₃/m*	*P6₃/m*
Symmetry	Hexagonal	Hexagonal	Hexagonal	Hexagonal	Hexagonal
a, Å	9.568431(5)	9.582288(8)	9.617445(2)	9.627483(2)	9.650372(3)
b, Å	9.568431(2)	9.582288(7)	9.617445(3)	9.627483(5)	9.650372(2)
c, Å	7.032033(4)	7.038839(2)	7.059281(4)	7.063548(7)	7.094781(5)
V, Å	557.562	559.719	565.471	566.995	572.213
Z	6	6	6	6	6
R_p	6.84	6.97	7.63	9.21	5.24
R_{wp}	9.35	9.83	10.65	11.54	7.71
χ^2	1.373	1.372	1.177	1.249	1.273

Table S2. Wyckoff Positions of Group *P63/m* (No. 176).

Multiplicity	Wyckoff letter	Site symmetry	Coordinates
12	i	1	(x,y,z) (-y,x-y,z) (-x+y,-x,z) (-x,-y,z+1/2) (y,-x+y,z+1/2) (x-y,x,z+1/2) (-x,-y,-z) (y,-x+y,-z) (x-y,x,-z) (x,y,-z+1/2) (-y,x-y,-z+1/2) (-x+y,-x,-z+1/2)
6	h	m..	(x,y,1/4) (-y,x-y,1/4) (-x+y,-x,1/4)(-x,-y,3/4) (y,-x+y,3/4) (x-y,x,3/4)
6	g	-1	(1/2,0,0) (0,1/2,0) (1/2,1/2,0) (1/2,0,1/2) (0,1/2,1/2) (1/2,1/2,1/2)
4	f	3..	(1/3,2/3,z) (2/3,1/3,z+1/2) (2/3,1/3,-z) (1/3,2/3,-z+1/2)
4	e	3..	(0,0,z) (0,0,z+1/2) (0,0,-z) (0,0,-z+1/2)
2	d	-6..	(2/3,1/3,1/4) (1/3,2/3,3/4)
2	c	-6..	(1/3,2/3,1/4) (2/3,1/3,3/4)
2	b	-3..	(0,0,0) (0,0,1/2)
2	a	-6..	(0,0,1/4) (0,0,3/4)

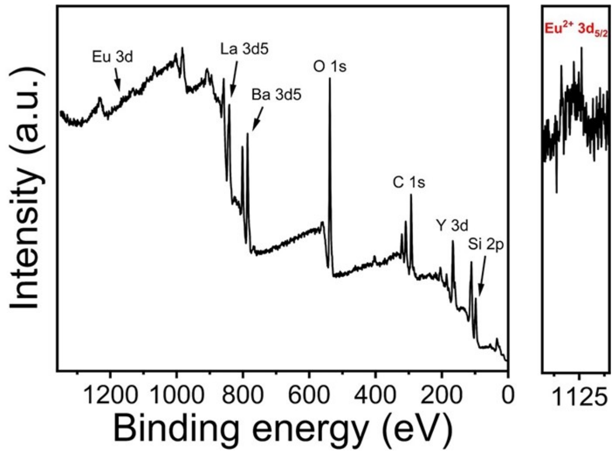

Figure S1. X-ray photoelectron spectroscopy (XPS) of $Ba_2Y_4La_4(SiO_4)_6O_2$:0.02Eu^{2+} phosphor, Figure on the right shows the high-resolution XPS spectrum of the Eu 3d core level of the sample.

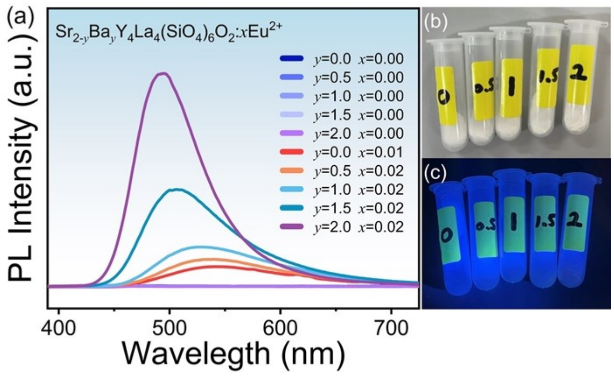

Figure S2. (a) Photoluminescence spectra of undoped Eu^{2+} samples and doped Eu^{2+}. (b) Images of the undoped Eu^{2+} sample under daylight illumination. (c) Images of the undoped Eu^{2+} samples under 365 nm UV light.

Table S3. Bond lengths in the $Ba_2Y_4La_4(SiO_4)_6O_2$:0.02Eu^{2+} compound.

Selected atoms	Bond length (Å)	Selected atoms	Bond length (Å)
Ba1-O1	2.469(7)	Ba2-O1	2.691(5)
Ba1-O1	2.469(7)	Ba2-O2	2.467(5)
Ba1-O1	2.468(7)	Ba2-O3	3.402(5)
Ba1-O2	2.526(6)	Ba2-O3	2.545(4)
Ba1-O2	2.527(6)	Ba2-O3	2.4142(16)
Ba1-O2	2.526(6)	Ba2-O3	3.402(5)
Ba1-O3	2.8749(15)	Ba2-O3	2.4142(16)
Ba1-O3	2.8739(15)	Ba2-O3	2.545(4)
Ba1-O3	2.8746(15)	Ba2-O4	2.287(5)
Y1-O1	2.469(7)	Y2-O1	2.691(5)
Y1-O1	2.469(7)	Y2-O2	2.467(5)
Y1-O1	2.468(7)	Y2-O3	2.4142(16)
Y1-O2	2.526(6)	Y2-O3	2.545(4)
Y1-O2	2.527(6)	Y2-O3	2.4142(16)
Y1-O2	2.526(6)	Y2-O3	2.545(4)
Y1-O3	2.8749(15)	Y2-O4	2.287(5)
Y1-O3	2.8739(15)	La2-O1	2.691(5)
Y1-O3	2.8746(15)	La2-O2	2.467(5)
La1-O1	2.469(7)	La2-O3	2.545(4)
La1-O1	2.469(7)	La2-O3	2.4142(16)
La1-O1	2.468(7)	La2-O3	2.545(4)
La1-O2	2.526(6)	La2-O3	2.4142(16)
La1-O2	2.527(6)	La2-O4	2.287(5)
La1-O2	2.526(6)		
La1-O3	2.8749(15)		
La1-O3	2.8739(15)		
La1-O3	2.8746(15)		
Average length (Å)	2.6232	Average length (Å)	2.5606

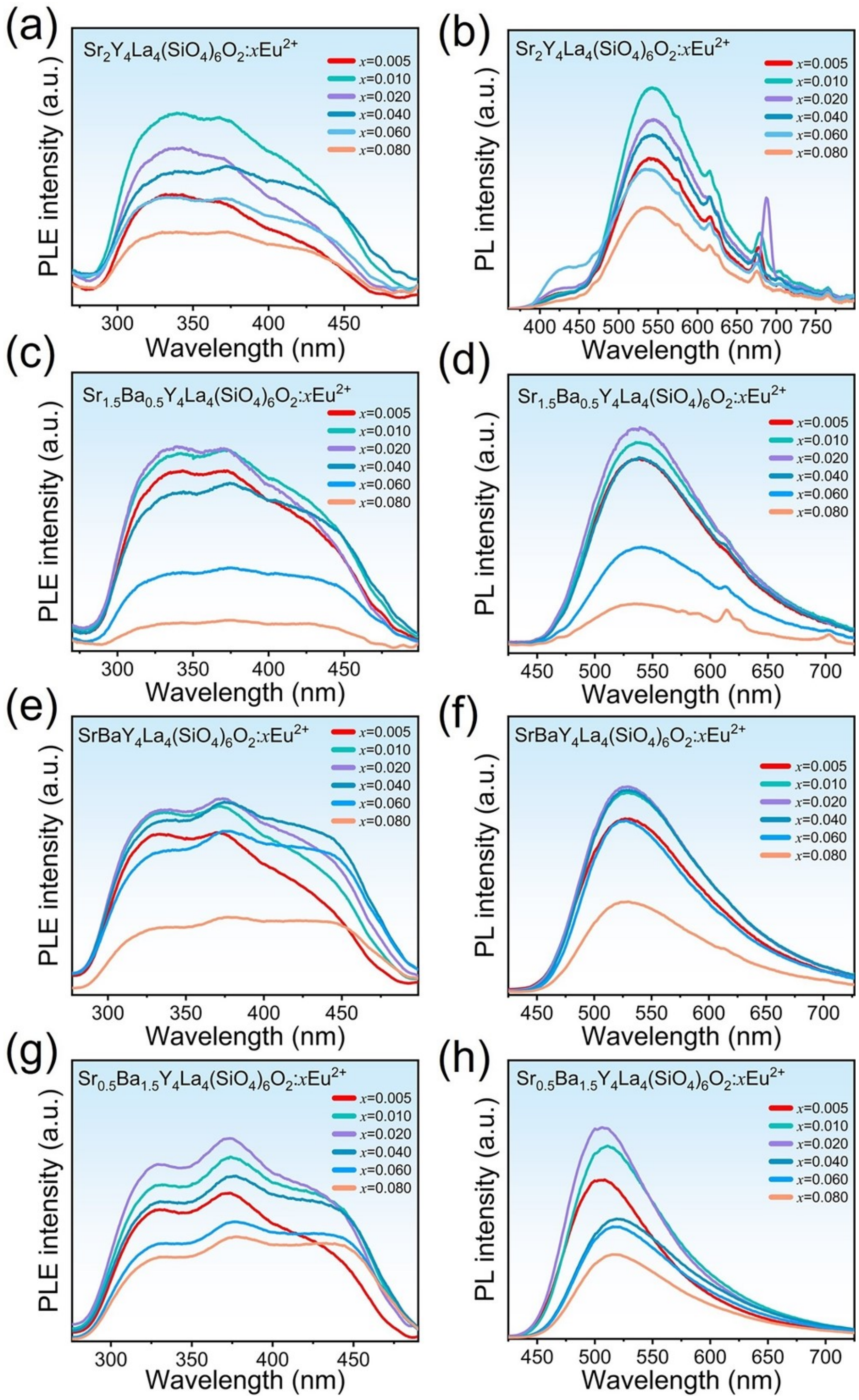

Figure S3. Concentration gradient (a) PLE and (b) PL spectra of $Sr_2Y_4La_4(SiO_4)_6O_2$:$x$$Eu^{2+}$ ($0.005 \leq x \leq 0.080$). Concentration gradient (c) PLE and (d) PL spectra of $Sr_{1.5}Ba_{0.5}Y_4La_4(SiO_4)_6O_2$:$x$$Eu^{2+}$($0.005 \leq x \leq 0.080$). Concentration gradient (e) PLE and (f) PL spectra of $SrBaY_4La_4(SiO_4)_6O_2$:$x$$Eu^{2+}$($0.005 \leq x \leq 0.080$) Concentration gradient (g) PLE and (h) PL spectra of $Sr_{0.5}Ba_{1.5}Y_4La_4(SiO_4)_6O_2$:$x$$Eu^{2+}$($0.005 \leq x \leq 0.080$).

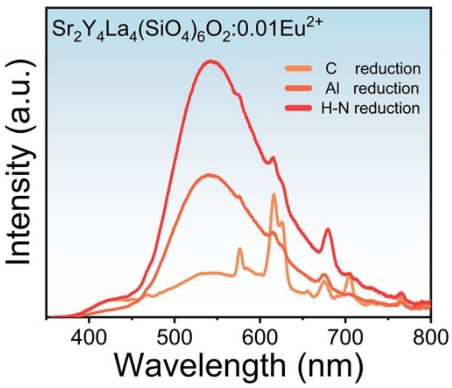

Figure S4. Photoluminescence spectra of $Sr_2Y_4La_4(SiO_4)_6O_2$:0.01Eu^{2+} samples under various reducing atmospheres.

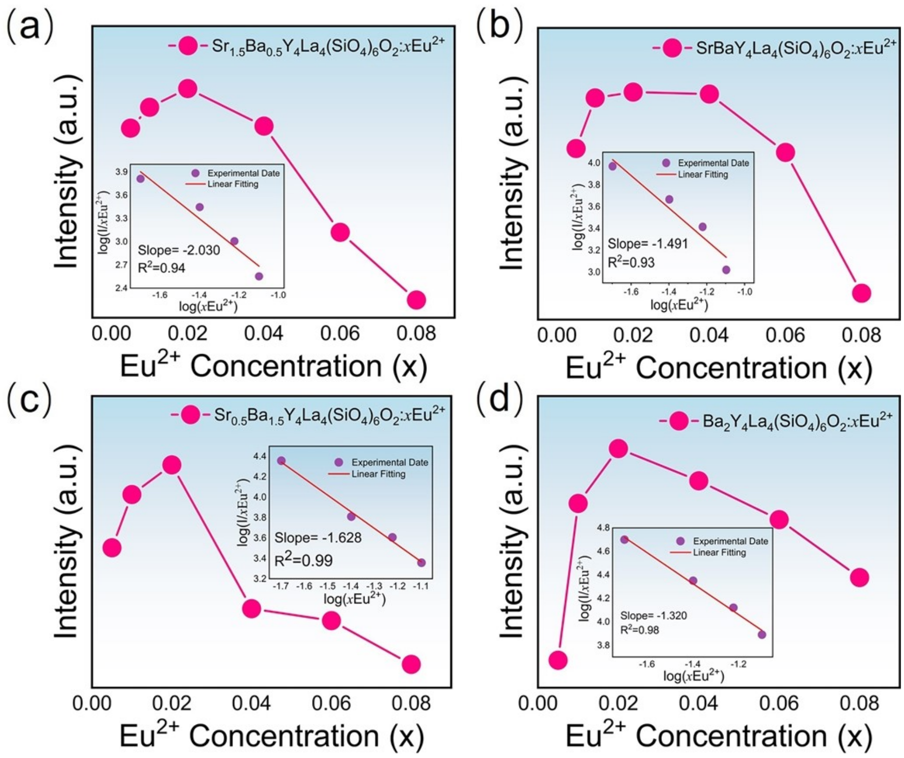

Figure S5. Emission intensity varies with increasing Eu^{2+} concentration x, inset shows the linear fitting of log(x) versus log(I/x) for phosphors with $x$$Eu^{2+}$ concentrations exceeding the quenching concentration of (a) $Sr_{1.5}Ba_{0.5}Y_4La_4(SiO_4)_6O_2$:$x$$Eu^{2+}$($0.005 \leq x \leq 0.080$), (b)$SrBaY_4La_4(SiO_4)_6O_2$:$x$$Eu^{2+}$($0.005 \leq x \leq 0.080$), (c) $Sr_{0.5}Ba_{1.5}Y_4La_4(SiO_4)_6O_2$:$x$$Eu^{2+}$($0.005 \leq x \leq 0.080$), (d) $Ba_2Y_4La_4(SiO_4)_6O_2$:$x$$Eu^{2+}$ ($0.005 \leq x \leq 0.080$).

Table S4. Slope obtained from the linear fitting of log(x) versus log(I/x) along with the calculated θ value for $Sr_2Y_4La_4(SiO_4)_6O_2$:$x$$Eu^{2+}$ ($0.005 \leq x \leq 0.080$), $Sr_{1.5}Ba_{0.5}Y_4La_4(SiO_4)_6O_2$:$x$$Eu^{2+}$ ($0.005 \leq x \leq 0.080$), $SrBaY_4La_4(SiO_4)_6O_2$:$x$$Eu^{2+}$ ($0.005 \leq x \leq 0.080$), $Sr_{0.5}Ba_{1.5}Y_4La_4(SiO_4)_6O_2$:$x$$Eu^{2+}$ ($0.005 \leq x \leq 0.080$), $Ba_2Y_4La_4(SiO_4)_6O_2$:$x$$Eu^{2+}$ ($0.005 \leq x \leq 0.080$).

Sample	Sr_2	$Sr_{1.5}Ba_{0.5}$	SrBa	$Sr_{0.5}Ba_{1.5}$	Ba_2
slope	-1.321	-2.030	-1.491	-1.628	-1.320
θ	3.963	6.090	4.473	4.884	3.960

Table S5. Gaussian deconvolution of the $Sr_{(2-y)}Ba_yY_4La_4(SiO_4)_6O_2$:$x$$Eu^{2+}$ ($0.005 \leq x \leq 0.08$, $0.5 \leq y \leq 2$) series of phosphors and their corresponding excitation and emission wavelengths.

y	Eu1(nm)	EuII(nm)	Ex1(nm)	Ex2(nm)	Em1(nm)	Em2(nm)
0.0	537	603	338	340	545	543
0.5	530	592	373	343	537	542
1.0	524	591	374	340	528	534
1.5	504	560	373	372	500	501
2.0	490	531	371	379	494	495

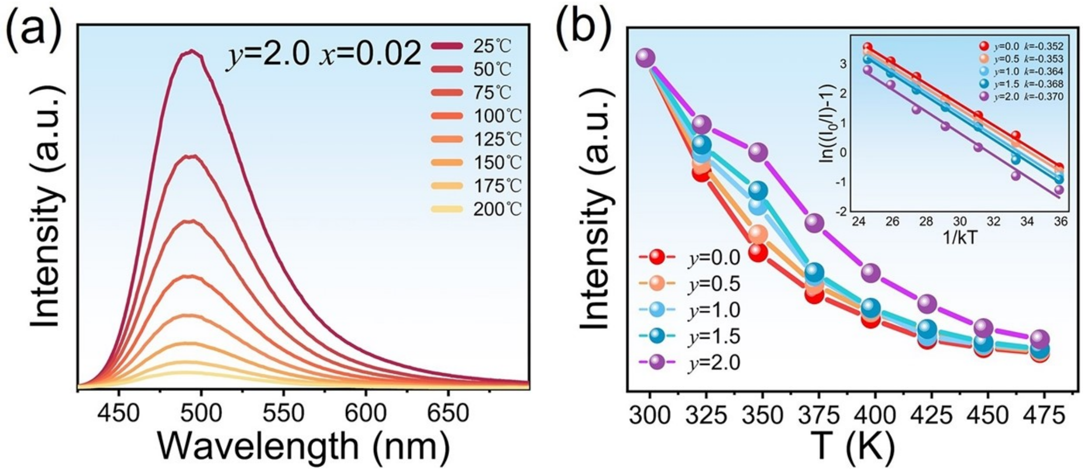

Figure S6. (a) Photoluminescence spectra of $Ba_2Y_4La_4(SiO_4)_6O_2$:0.02Eu^{2+} phosphors in the temperature range of 25-200°C. (b) Relationship between luminescence intensity and temperature for the $Sr_{(2-y)}Ba_yY_4La_4(SiO_4)_6O_{2:}Eu^{2+}$ ($0.005 \leq x \leq 0.08$, $0.5 \leq y \leq 2$) series of phosphors, the inset shows the relationship between ln((I_0/I)-1) and *1/kT* for the $Sr_{(2-y)}Ba_yY_4La_4(SiO_4)_6O_{2:}Eu^{2+}$ ($0.005 \leq x \leq 0.08$, $0.5 \leq y \leq 2$) series of phosphors.

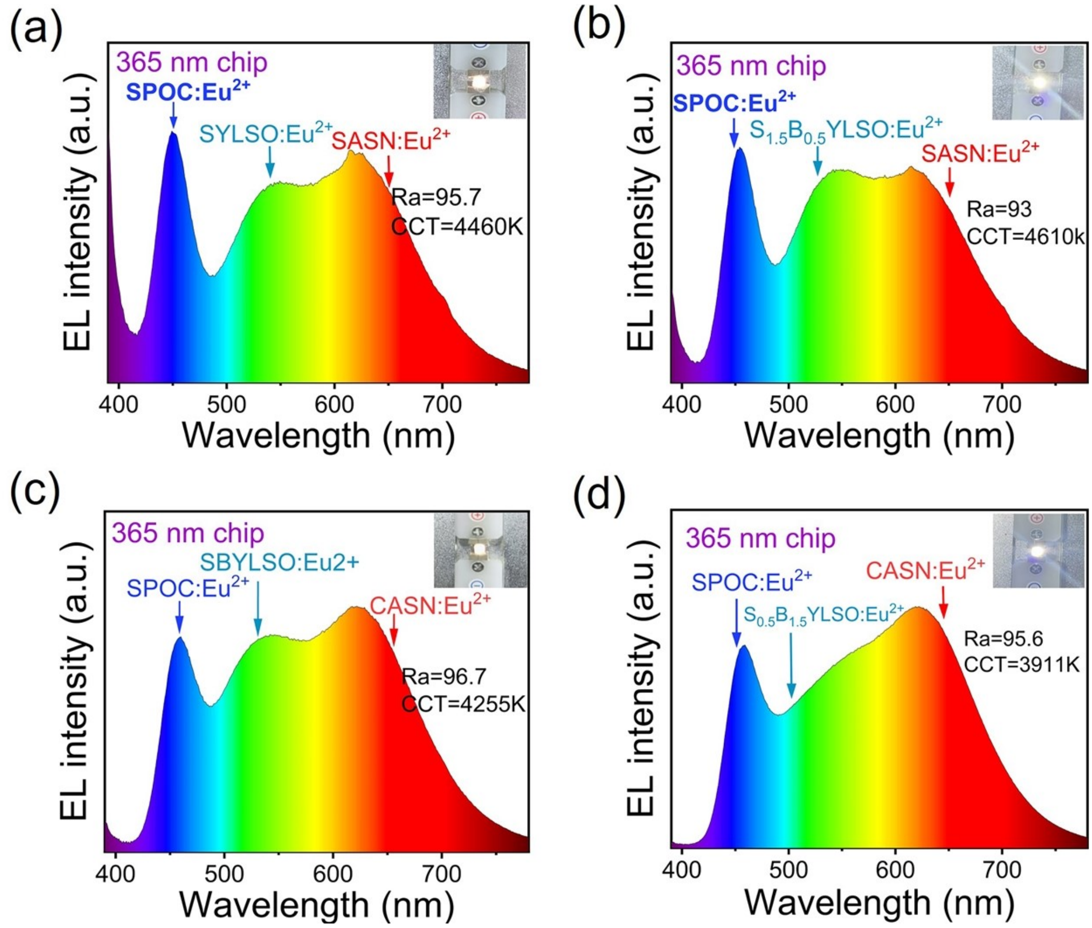

Figure S7. EL spectra of devices fabricated by uniformly mixing the prepared yellow phosphors (a) $Sr_2Y_4La_4(SiO_4)_6O_2$:0.01Eu^{2+} / (b) $Sr_{1.5}Ba_{0.5}Y_4La_4(SiO_4)_6O_2$:0.02$Eu^{2+}$ / (c) $SrBaY_4La_4(SiO_4)_6O_2$:0.01Eu^{2+}, and / (d) yellow-green phosphor $Sr_{0.5}Ba_{1.5}Y_4La_4(SiO_4)_6O_2$:0.01$Eu^{2+}$ with commercial blue phosphors $Sr_5(PO_4)_3Cl$:Eu^{2+} (SPOC:Eu^{2+}) and commercial red phosphors $CaAlSiN_3$:Eu^{2+} (CASN:Eu^{2+}) and then coating them onto 365 nm chips, inset displays a photograph of the packaged WLED under illumination.

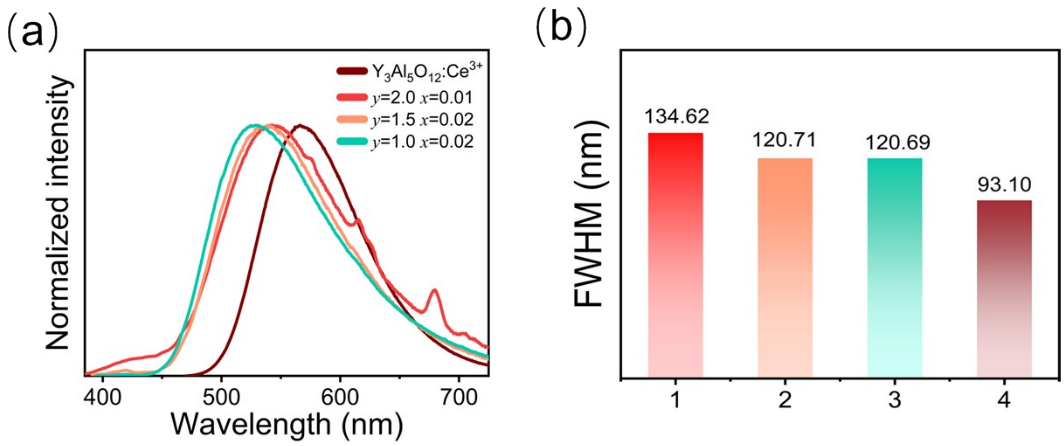

Figure S8. (a) Normalized spectral diagrams of $Sr_2Y_4La_4(SiO_4)_6O_2$:0.01Eu^{2+}, $Sr_{1.5}Ba_{0.5}Y_4La_4(SiO_4)_6O_2$:0.02$Eu^{2+}$, $SrBaY_4La_4(SiO_4)_6O_2$:0.02Eu^{2+} and $Y_3Al_5O_{13}:Ce^{3+}$. (b) full-width at half-maximum (FWHM) of the spectra of $Sr_2Y_4La_4(SiO_4)_6O_2$:0.01Eu^{2+}, $Sr_{1.5}Ba_{0.5}Y_4La_4(SiO_4)_6O_2$:0.02$Eu^{2+}$, $SrBaY_4La_4(SiO_4)_6O_2$:0.02Eu^{2+} and $Y_3Al_5O_{13}:Ce^{3+}$.

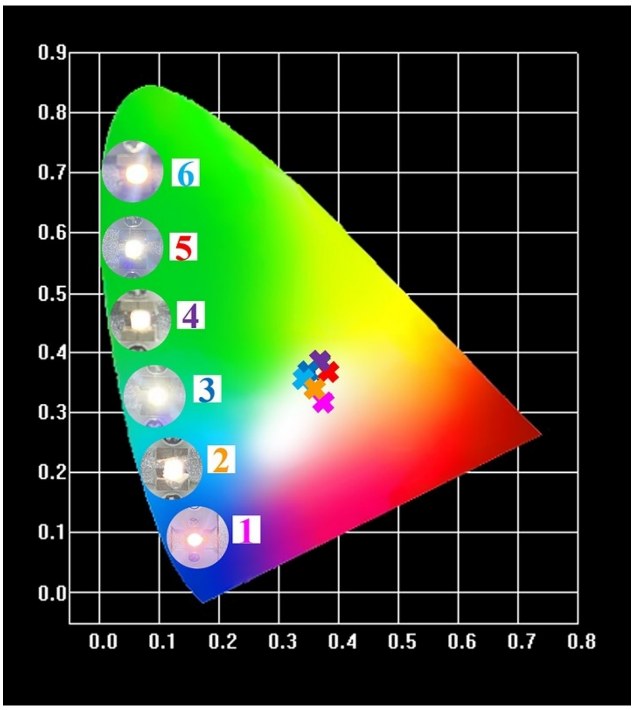

Figure S9. Emission positions of devices (1-6) WLED(0), WLED(Sr_2), WLED($Sr_{1.5}$), WLED(Sr_1), WLED($Sr_{0.5}$), and WLED(Ba_2), in the CIE diagram.